

# Stepwise Synthesis of Metal–Organic Frameworks: Replacement of Structural Organic Linkers

Brandon J. Burnett,<sup>†</sup> Paul M. Barron,<sup>†</sup> Chunhua Hu,<sup>‡</sup> and Wonyoung Choe<sup>\*,†,§</sup>

<sup>†</sup>Department of Chemistry and <sup>§</sup>Nebraska Center for Materials and Nanoscience, University of Nebraska-Lincoln, Lincoln, Nebraska 68588-0304, United States

<sup>‡</sup>Department of Chemistry, New York University, New York, New York 10003-6688, United States

 Supporting Information

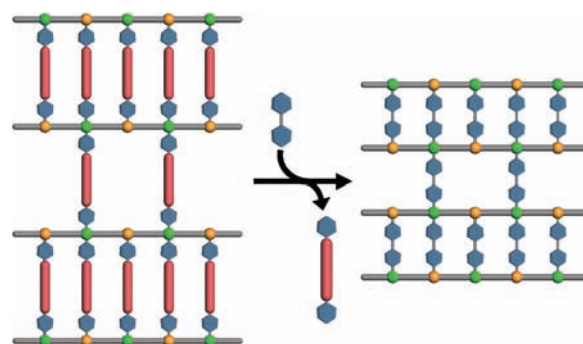
**ABSTRACT:** We demonstrate how a single-crystal to single-crystal transformation resulting from bridging-linker replacement is possible in extended 2D and 3D metal–organic frameworks (MOFs) by introducing pillared paddlewheel MOF structures into a solution containing dipyridyl linkers. No lateral movement of the layers was observed during this transformation, creating a templating effect from the “parent” structure to the “daughter” structure. A previously unattainable structure was obtained by a two-step synthetic method utilizing the bridging-linker replacement transformation method. Additionally, a bridging-linker insertion was observed when excess linker was used with the 2D MOF structure, inducing an overall 2D to 3D transformation.

Examples of metal–organic materials (MOMs) are metal–organic frameworks (MOFs) and metal–organic polyhedra (MOPs), both of which are self-assembled from two types of structural components, namely, metal nodes and organic linkers. Through changes in the metal nodes or organic linkers used in the synthesis of MOMs, the topology can be tuned to optimize desired properties in applications such as gas storage, catalysis, and molecular sensing.<sup>1–4</sup>

Traditionally, MOMs are assembled in “one-pot” solvothermal syntheses in which topology control is accomplished only by careful selection of the metal, organic linker, and synthetic conditions.<sup>5,6</sup> Although great success has been obtained through this simple synthetic route, more sophisticated synthetic strategies have recently emerged through stepwise reactions, which may lead to complex, multifunctional MOMs.<sup>7–15</sup> These strategies involve altering either (1) the metal node or (2) the organic linker after initial crystallization. In the first strategy, metal nodes that are integral parts of the structure can be exchanged, as demonstrated by Kim.<sup>7</sup> His group reported exchange of Cd<sup>2+</sup> ions in the Cd<sub>4</sub>O metal nodes with Pb<sup>2+</sup> ions in a single-crystal to single-crystal transformation.<sup>7</sup>

Among several approaches that involve altering the organic linkers of MOMs, perhaps the most common one is modification of the functional group in the organic linker after the initial reaction while keeping the same framework topology. This post-synthetic modification (PSM) approach, later coined by Cohen,<sup>8</sup> was first conceived by Hoskins and Robson<sup>9</sup> and demonstrated a decade later by Lee and co-workers,<sup>10</sup> who treated an alcohol functional group of the linker trifluoroacetic anhydride to form

**Scheme 1. Schematic Representation of Bridging-Linker Replacement in an Extended MOF**



an ester.<sup>10</sup> Recently, the groups of Cohen, Yaghi, and many others have decorated the pore surfaces of MOFs for applications including catalysis and superhydrophobicity.<sup>11</sup> A second approach is insertion of new linkers into MOMs. The Kitagawa and Chen groups have inserted bidentate bridging linkers into 2D MOFs with accessible metal centers, resulting in structural transformations to 3D MOFs.<sup>12,13</sup> Zhou reported another structural transformation from a 0D MOP to a 3D MOF by insertion of pillaring bipyridyl linkers.<sup>14</sup> An interesting new approach to changing the organic linkers is *replacement* of the structure-building organic linkers. This replacement concept has been widely used in discrete organic and organometallic species but seldom in MOM synthesis. Recently, Zhou successfully demonstrated such replacement reactions using MOPs, forming an isotreticular series with various pore sizes, shapes, and functionalities.<sup>15</sup>

To date, however, this replacement concept has not been extended to infinite 2D or 3D MOFs. We hypothesized that replacement of bridging linkers should also be possible in multidimensional (i.e., 2D or 3D) MOFs. In this communication, we report two cases of replacement reactions of structure-building linkers in 2D and 3D MOF systems that result in single-crystal to single-crystal transformations (see Scheme 1). To our knowledge, these are the first examples of linker-replacement reactions in multidimensional MOFs. Additionally, we report a 2D to 3D transformation that occurs via a linker-insertion mechanism upon the introduction of excess linkers.

**Received:** March 3, 2011

**Published:** June 15, 2011

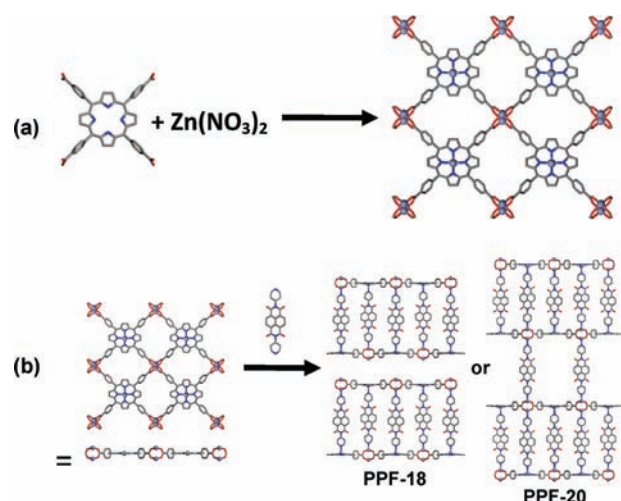


**Figure 1.** (a) 2D grid motif based on a porphyrin building block and zinc paddlewheel metal node.<sup>16a</sup> (b) 2D bilayer and 3D frameworks synthesized by initial “one-pot” syntheses with different stoichiometric amounts of the bridging linker DPNI.<sup>17</sup> Hydrogen atoms and solvent molecules have been omitted for clarity.

We previously reported a series of porphyrin paddlewheel frameworks (PPFs) based on the 2D square-grid layer motif constructed from tetrakis(4-carboxyphenyl)porphyrin (TCPP) and the  $Zn_2(COO)_4$  paddlewheel metal node.<sup>16,17</sup> The 2D layers can be connected in the third dimension by coordinating the metal centers within the paddlewheels and inside the porphyrin rings with dipyrindyl bridging linkers (Figure 1).<sup>17</sup> We speculated that pillared paddlewheel frameworks could be suitable candidates for investigating the bridging-linker exchange transformation because the axial metal–nitrogen bonds are relatively weaker than the metal–oxygen bonds in pillared paddlewheel frameworks.<sup>18</sup> To demonstrate the bridging-linker replacement, two PPF structures, 2D PPF-18 and 3D PPF-20, were synthesized as “parent” structures to test our hypothesis.

PPF-18 and PPF-20 were synthesized via solvothermal reactions of TCPP,  $Zn(NO_3)_2 \cdot 6H_2O$ , and the bridging linker *N,N'*-di-4-pyridyl naphthalenetetracarboxydiimide (DPNI) at 80 °C for 24 h, following the published method.<sup>17</sup> PPF-18 is a 2D bilayer structure in which the porphyrin paddlewheel layers are stacked in an AB fashion, creating *P4/nmm* symmetry (Figure 1).<sup>17</sup> The zinc atoms in the porphyrin cores are pentacoordinated, whereas the  $Zn_2(COO)_4$  paddlewheels are axially coordinated by solvent molecules between the bilayers. PPF-20 is a 3D structure in which the porphyrin paddlewheel layers are stacked in an ABBA fashion, creating *I4/mmm* symmetry (Figure 1).<sup>17</sup>

For the replacement reaction, crystals of PPF-18 were filtered and washed in *N,N*-diethyl formamide (DEF) and then introduced into a DEF/EtOH solution containing 4,4'-bipyridine (BPY) as the replacement linker and left to exchange for 2 h. During this time, BPY entered into the pores of PPF-18 and replaced the DPNI linkers. As shown in Figure 2a, a new phase, PPF-27, was obtained and confirmed by powder X-ray diffraction (PXRD) [see the Supporting Information (SI)]. Single-crystal X-ray diffraction data were obtained for PPF-27.<sup>19</sup> PPF-27 retains the *P4/nmm* symmetry of PPF-18, but the distance between layers in the bilayer is reduced from 21.2 to 12.8 Å. The unit cell volume is also reduced from 8630 to 5793 Å<sup>3</sup>. Interestingly, the

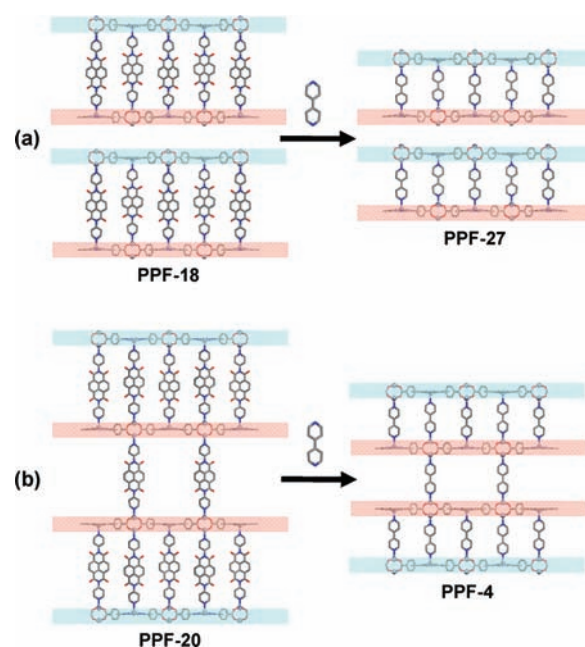


**Figure 2.** Introduction of the bridging linker BPY to crystals of (a) PPF-18 and (b) PPF-20, transforming them to PPF-27 and PPF-4, respectively. Blue and pink bands represent “A” and “B” layers, respectively. The AB and ABBA topologies in PPF-18 and PPF-20 are retained in PPF-27 and PPF-4, respectively, showing a templating effect.

BPY-linked bilayer structure has not been reported to date in PPFs because of difficulties in synthesis.<sup>17</sup> With the traditional “one-pot” solvothermal synthesis, the bilayer was only a secondary phase together with major-phase PPF-4 structure. To obtain PPF-27 as a single phase, this two-step strategy via bridging-linker replacement was advantageous. When excess amounts of BPY (>2 equiv) were added to the reaction mixture, a second phase was observed by PXRD. Additional BPY linkers coordinate to the open paddlewheels between the bilayers, resulting in the formation of the further coordinated ABBA-stacked 3D PPF-4 phase, a MOF previously reported by our group.<sup>16</sup> Single-phase PPF-4 was obtained when the amount of BPY was increased to 4 equiv, as confirmed by PXRD (see the SI).

To further demonstrate the utility of this linker-replacement transformation on 3D systems, crystals of PPF-20 were introduced into a DEF/EtOH solution containing excess BPY ligands and left to exchange for 2 h, similar to the case for PPF-18. Single-phase PPF-4 (Figure 2b) was obtained, as confirmed by PXRD (see the SI). The *c* parameters in PPF-20 and PPF-4 are 87.68 and 54.24 Å, respectively, showing the contraction in the *c* parameter upon replacement of the bridging linker. This process was also monitored by a series of UV-vis spectra of the solution as the replacement proceeded. The DPNI bridging linker, like many naphthalenediimides, shows absorption bands in the UV range,<sup>20</sup> and an increasing signal due to DPNI was observed as a function of time. This signal was then converted to concentration of DPNI linker and used to estimate the percent transformation versus time (see Figure S24 in the SI). On the basis of this estimation, the transformation was 97% accomplished after 2 h.

Single-crystal to single-crystal experiments were performed for both the 2D and 3D systems, following the method reported by Suh,<sup>21</sup> confirming a solid to solid mechanism and excluding the possibility of a dissolution/recrystallization mechanism.

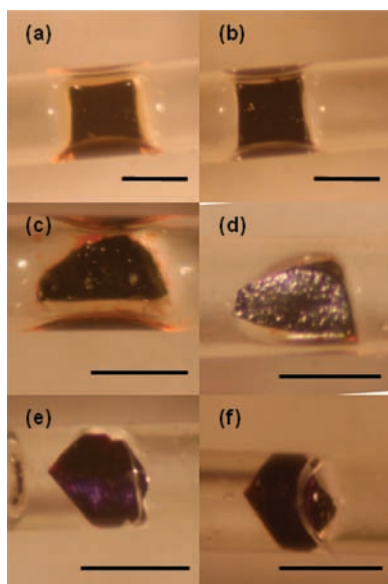


**Figure 3.** Photographs of PPF crystals in single-crystal to single-crystal transformation. (a) PPF-18 crystal before transformation. (b) After immersion in BPY solution overnight to afford PPF-27. (c) PPF-18 crystal before transformation. (d) After immersion in BPY solution overnight to afford PPF-4. (e) PPF-20 crystal before transformation. (f) After immersion in BPY solution overnight to afford PPF-4. The scale bar in the figures represents 300  $\mu\text{m}$ .

Single crystals of PPF-18 and PPF-20 were selected and inserted into a 0.3 mm capillary tube. Photographs were taken before the transformation (Figure 3), and the unit cell parameters were measured and compared to the unit cell parameters obtained from the solved single-crystal structures (Tables S2–S4 in the SI). The single crystals were then introduced to a BPY solution and left to react overnight. The resulting single crystals were photographed to show the overall shape retention during the transformation (Figure 3). The unit cell parameters were measured and compared to the those of the daughter structure obtained from single-crystal data. PPF-18 [ $a = b = 16.718(8)$  Å,  $c = 31.36(5)$  Å] was transformed into PPF-27 [ $a = b = 16.704(2)$  Å,  $c = 20.86(4)$  Å] (Figure 3a,b, respectively). PPF-18 [ $a = b = 16.709(9)$  Å,  $c = 31.21(6)$  Å] was transformed into PPF-4 [ $a = b = 16.722(6)$  Å,  $c = 54.38(4)$  Å] (Figure 3c,d, respectively). PPF-20 [ $a = b = 16.727(2)$  Å,  $c = 87.59(5)$  Å] was transformed into PPF-4 [ $a = b = 16.706(6)$  Å,  $c = 54.89(3)$  Å] (Figure 3e,f, respectively). The presence of DPNI linkers stuck in the pores after each transformation was probed by solution  $^1\text{H}$  NMR and UV–vis spectroscopy of acid-digested samples following the method reported by Cohen.<sup>22</sup> For each of the systems, no residual DPNI linkers were observed in either the  $^1\text{H}$  NMR or UV–vis spectra (see the SI). The reverse replacement reactions were attempted for both the 2D and 3D systems, but no transformations were observed by PXRD, indicating that the coordination equilibrium favors coordination to BPY over DPNI.<sup>23</sup>

An interesting templating effect was also observed in both the 2D and 3D systems during this linker-replacement transformation (Figure 2). There was no lateral shift in the 2D porphyrin paddlewheel layers during the replacement, allowing retention of the parent stacking sequence in the daughter structure, as exemplified by the PPF-18  $\rightarrow$  PPF-27 transformation when

there was a limited amount of BPY in solution. When the parent structure (PPF-18) was stacked in an AB fashion, the daughter (PPF-27) retained this stacking sequence. We also noticed a similar trend in the PPF-20  $\rightarrow$  PPF-4 transformation, where the ABBA stacking pattern of the parent was conserved in the daughter (Figure 2b). One can imagine that the ABBA PPF-4 structure can be synthesized from the PPF-27 bilayer structure through lateral movement. When excess BPY linkers were inserted, the AB bilayer system shifted laterally, similar to other known cases for 2D paddlewheel MOFs.<sup>24</sup> The paddlewheel metal nodes coordinated further to create the ABBA structure.<sup>25</sup>

In both the 2D and 3D replacement reactions, the porous nature of these MOFs facilitates the transformation.<sup>26</sup> Dipyriddy bridging linkers have the ability to diffuse into the interior of these MOFs, as shown by Connolly surface models (see the SI). There they can access the internal metal centers and replace the existing linkers even when those linkers are structurally integral to these MOFs. The linkers from the parent structure then can diffuse out of the structure, as seen in the UV–vis experiment and modeled by Connolly surface models (see the SI). This bridging-ligand replacement in multidimensional MOFs demonstrates the dynamic nature of the internal compartment of MOFs in the solid state. Such a phenomenon is rather remarkable. A common assumption has been that extended solids cannot be used as starting materials for stepwise reactions because these solids are insoluble in solution. However, these two systems, PPF-18 and PPF-20, show that a replacement synthesis can indeed be accomplished even with crystalline solid intermediates, as evidenced by the single-crystal to single-crystal experiments and supported by the UV–vis experiment.<sup>25</sup> The UV–vis data showed that only a trace amount of porphyrin (0.65%) broke from the structure and went into solution during the transformation (see the SI), confirming that the overall 2D porphyrin paddlewheel structure stayed intact.

The Kitagawa group recently demonstrated that surface pyridyl or carboxylate ligands can be replaced, creating a monolayer on the outside of the crystals.<sup>23</sup> Our work shows that this concept can also be used to transform the whole MOF structure. Epitaxial growth of MOFs (i.e., MOF@MOF structures) has also been demonstrated by incorporating different synthetic procedures. These MOF@MOF structures were obtained by introducing seed crystals into a solution containing additional ligands and metal ions.<sup>27</sup> In contrast, in our synthesis, the crystals were filtered and washed to remove any excess metals in solution, and no metal was added to coordinate to additional solution ligands, thereby promoting the linker replacement and suppressing the epitaxial growth mechanism.

In summary, we have demonstrated how bridging-ligand replacement can be applied to two cases of extended 2D and 3D MOFs. Because of the porous nature of these MOFs, dipyriddy linkers can diffuse into the interiors of the MOFs and replace the existing structural dipyriddy struts. The stacking patterns of the parent structures were maintained throughout the transformations, showing a templating effect. Such linker replacement can also be utilized in a stepwise synthesis, despite the fact that these MOFs are insoluble in solution. The development of replacement reactions in MOFs is not limited to the synthesis of single-phase materials that are otherwise unattainable, as seen with PPF-27 in this study. Rather, the replacement reaction in MOFs, together with other stepwise synthetic approaches, can offer a new avenue for manipulating MOFs in the pursuit of constructing complex architectures designed for specific functions.

We expect that there will be many more multidimensional MOF systems that exhibit similar linker replacement.

## ■ ASSOCIATED CONTENT

**S Supporting Information.** Synthetic conditions, PXRD setup and patterns, single-crystal to single-crystal data, acid digestion data, a CIF file for PPF-27, TGA data, crystallographic data, and UV–vis spectra. This material is available free of charge via the Internet at <http://pubs.acs.org>.

## ■ AUTHOR INFORMATION

### Corresponding Author

choe2@unl.edu

## ■ ACKNOWLEDGMENT

The authors gratefully acknowledge the University of Nebraska-Lincoln for funding and support.

## ■ REFERENCES

- (1) For reviews of MOFs, see: (a) Tranchemontagne, D. J.; Mendoza-Cortés, J. L.; O’Keeffe, M.; Yaghi, O. M. *Chem. Soc. Rev.* **2009**, *38*, 1257. (b) Yaghi, O. M.; O’Keeffe, M.; Ockwig, N. W.; Chae, H. K.; Eddaoudi, M.; Kim, J. *Nature* **2003**, *423*, 705. (c) Eddaoudi, M.; Kim, J.; Rosi, N. L.; Vodak, D.; Wachter, J.; O’Keeffe, M.; Yaghi, O. M. *Science* **2002**, *295*, 469. (d) Moulton, B.; Zaworotko, M. *Chem. Rev.* **2001**, *101*, 1629.
- (2) (a) Murray, L. J.; Dincă, M.; Long, J. R. *Chem. Soc. Rev.* **2009**, *38*, 1294. (b) Collins, D. J.; Zhou, H.-C. *J. Mater. Chem.* **2007**, *17*, 3154. (c) Farha, O. K.; Oezguer, Y. A.; Eryazici, I.; Malliakas, C. D.; Hauser, B. G.; Kanatzidis, M. G.; Nguyen, S. T.; Snurr, R. Z.; Hupp, J. T. *Nat. Chem.* **2010**, *2*, 944.
- (3) (a) Ma, L.; Abney, C.; Lin, W. *Chem. Soc. Rev.* **2009**, *38*, 1248. (b) Lee, J.; Farha, O. K.; Roberts, J.; Scheidt, K. A.; Nguyen, S. T.; Hupp, J. T. *Chem. Soc. Rev.* **2009**, *38*, 1450. (c) Seo, J. S.; Whang, D.; Lee, H.; Jun, S. I.; Oh, J.; Jeon, Y. J.; Kim, K. *Nature* **2000**, *404*, 982. (d) Liqing, M.; Falkowski, J. M.; Abney, C.; Lin, W. *Nat. Chem.* **2010**, *2*, 838.
- (4) (a) Allendorf, M. D.; Bauer, D. A.; Bhakta, R. K.; Houk, R. J. T. *Chem. Soc. Rev.* **2009**, *38*, 1330. (b) Lan, A.; Li, K.; Wu, H.; Olson, D. H.; Emge, T. J.; Ki, W.; Hong, M.; Li, J. *Angew. Chem., Int. Ed.* **2009**, *48*, 2334. (c) Odbadrakh, K.; Lewis, J. P.; Nicholson, D. M. *J. Phys. Chem. C* **2010**, *114*, 7535.
- (5) In contrast, discrete molecules and organometallic species have been manipulated for decades by organic and inorganic chemists via step-by-step synthetic strategies.
- (6) For an example of a complex hierarchical MOF assembled via “one-pot” synthesis, see: Sudik, A. C.; Côté, A. P.; Wong-Foy, A. G.; O’Keeffe, M.; Yaghi, O. M. *Angew. Chem., Int. Ed.* **2006**, *45*, 2528.
- (7) Das, S.; Kim, H.; Kim, K. *J. Am. Chem. Soc.* **2009**, *131*, 3814.
- (8) For reviews of postsynthetic modification, see: (a) Wang, Z.; Cohen, S. M. *Chem. Soc. Rev.* **2009**, *38*, 1315. (b) Tanabe, K. K.; Cohen, S. M. *Chem. Soc. Rev.* **2011**, *40*, 498. (c) Cohen, S. M. *Chem. Sci.* **2010**, *1*, 32. (d) Song, Y.-F.; Cronin, L. *Angew. Chem., Int. Ed.* **2008**, *47*, 4635.
- (9) Hoskins, B. F.; Robson, R. J. *Am. Chem. Soc.* **1990**, *112*, 1546.
- (10) Kiang, Y.-H.; Gardner, G. B.; Lee, S.; Xu, Z.; Lobkovsky, E. *J. Am. Chem. Soc.* **1999**, *121*, 8204.
- (11) (a) Nguyen, J. G.; Cohen, S. M. *J. Am. Chem. Soc.* **2010**, *132*, 4560. (b) Tanabe, K. K.; Cohen, S. M. *Angew. Chem., Int. Ed.* **2009**, *48*, 7424. (c) Oisaki, K.; Li, Z.; Furukawa, H.; Czaja, A. U.; Yaghi, O. M. *J. Am. Chem. Soc.* **2010**, *132*, 9262.
- (12) Kitaura, R.; Iwahori, F.; Matsuda, R.; Kitagawa, S.; Kubota, Y.; Takata, M.; Kobayashi, T. C. *Inorg. Chem.* **2004**, *43*, 6522.
- (13) Chen, Z.; Xiang, S.; Zhao, D.; Chen, B. *Cryst. Growth Des.* **2009**, *9*, 5293.
- (14) (a) Li, J.-R.; Timmons, D. J.; Zhou, H.-C. *J. Am. Chem. Soc.* **2009**, *131*, 6368. (b) Zaworotko, M. J. *Nat. Chem.* **2009**, *1*, 267.
- (15) Li, J.-R.; Zhou, H.-C. *Nat. Chem.* **2010**, *2*, 893.
- (16) (a) Choi, E.-Y.; Wray, C. A.; Hu, C.; Choe, W. *CrystEngComm* **2009**, *11*, 553. (b) Choi, E.-Y.; Barron, P. M.; Novotny, R. W.; Son, H.-T.; Hu, C.; Choe, W. *Inorg. Chem.* **2009**, *48*, 426.
- (17) Chung, H.; Barron, P. M.; Novotny, R. W.; Son, H.-T.; Hu, C.; Choe, W. *Cryst. Growth Des.* **2009**, *9*, 3327.
- (18) The binding energies for Zn–N and Zn–O were estimated to be 150 and 360 kJ/mol, respectively (see ref 1a).
- (19) For crystallographic data for PPF-27, see the SI.
- (20) (a) Ozser, M. E.; Uzun, D.; Elci, I.; Icil, H.; Demuth, M. *Photochem. Photobiol. Sci.* **2003**, *2*, 218. (b) Erten, Ş.; Posokhov, Y.; Alp, S.; İçli, S. *Dyes Pigm.* **2005**, *64*, 171.
- (21) Choi, H. J.; Suh, M. P. *J. Am. Chem. Soc.* **2004**, *126*, 15844.
- (22) Wang, Z.; Tanabe, K. K.; Cohen, S. M. *Inorg. Chem.* **2009**, *48*, 296.
- (23) Kondo, M.; Furukawa, S.; Hirai, K.; Kitagawa, S. *Angew. Chem., Int. Ed.* **2010**, *49*, 5327.
- (24) Lateral movement of a paddlewheel framework was previously observed by Kitagawa and co-workers.<sup>12</sup>
- (25) This phenomenon has also been seen in the intercalation chemistry of layered double hydroxide (LDH) compounds. O’Hare reported a similar transformation in the Zn<sub>2</sub>Cr LDH system: upon introduction of excess adipate anions, first the succinate and tartrate anions were replaced, after which adipate further replaced the Cl<sup>−</sup> anions in the remaining layers (see: Feng, Y. J.; Williams, G. R.; Lerous, F.; Tavio-Gueho, C.; O’Hare, D. *Chem. Mater.* **2006**, *18*, 4312). This report, however, provided only PXRD data to support their discussion. The use of MOFs has enabled us to report single-crystal information on this phenomenon. Herein we have reported transformations in which a longer linker is replaced with a shorter linker, resulting in a contraction between layers. Interestingly, O’Hare’s report indicates that similar transformations involving replacement of a shorter linker with a longer linker could happen, as seen from the replacement of the shorter succinate and tartrate anions with the longer adipate anion.
- (26) Porosity is conventionally defined by two parameters: demonstration of permeability and retention of structure upon guest removal/exchange (see: Barbour, L. J. *Chem. Commun.* **2006**, 1163). The observation of pillar molecules moving into solution during the transformation indicates the permeability of the structure, similar to reports in which porosity was proved by inclusion of dye molecules into the crystal, as demonstrated by Lin (see: Ma, L.; Lin, W. *J. Am. Chem. Soc.* **2008**, *130*, 13834). The 2D square-grid layers retained their structure during the transformation, as exemplified by the templating effect. Had the structure fully dissolved and recrystallized, contamination by either 2D or 3D species would be evident in the PXRD pattern.
- (27) (a) Koh, K.; Wong-Foy, A. G.; Matzger, A. J. *Chem. Commun.* **2009**, 6162. (b) Furukawa, S.; Hirai, K.; Nakagawa, K.; Takashima, Y.; Matsuda, R.; Tsuruoka, T.; Kondo, M.; Haruki, R.; Tanaka, D.; Sakamoto, H.; Shimomura, S.; Sakata, O.; Kitagawa, S. *Angew. Chem., Int. Ed.* **2009**, *48*, 1766. (c) Furukawa, S.; Hirai, K.; Takasima, Y.; Nakagawa, K.; Kondo, M.; Tsuruoka, T.; Sakata, O.; Kitagawa, S. *Chem. Commun.* **2009**, 5097.